



**HAL**  
open science

## The consumption of ice-derived resources is associated with higher mercury contamination in an Arctic seabird

Fanny Cusset, Julie Charrier, Guillaume Massé, Mark Mallory, Birgit Braune, Jennifer Provencher, Gaël Guillou, Philippe Massicotte, Jérôme Fort

### ► To cite this version:

Fanny Cusset, Julie Charrier, Guillaume Massé, Mark Mallory, Birgit Braune, et al.. The consumption of ice-derived resources is associated with higher mercury contamination in an Arctic seabird. *Environmental Research*, 2023, 238, pp.117066. 10.1016/j.envres.2023.117066 . hal-04223391

**HAL Id: hal-04223391**

**<https://hal.science/hal-04223391>**

Submitted on 21 Nov 2023

**HAL** is a multi-disciplinary open access archive for the deposit and dissemination of scientific research documents, whether they are published or not. The documents may come from teaching and research institutions in France or abroad, or from public or private research centers.

L'archive ouverte pluridisciplinaire **HAL**, est destinée au dépôt et à la diffusion de documents scientifiques de niveau recherche, publiés ou non, émanant des établissements d'enseignement et de recherche français ou étrangers, des laboratoires publics ou privés.

# 1 **The consumption of ice-derived resources is associated with** 2 **higher mercury contamination in an Arctic seabird**

3 Fanny Cusset<sup>1,2,a\*</sup>, Julie Charrier<sup>2,a\*</sup>, Guillaume Massé<sup>1,3</sup>, Mark Mallory<sup>4</sup>, Birgit Braune<sup>5</sup>, Jennifer  
4 Provencher<sup>5</sup>, Gaël Guillou<sup>2</sup>, Philippe Massicotte<sup>1</sup> and Jérôme Fort<sup>2</sup>

5

6 <sup>1</sup> Takuvik International Research Laboratory (IRL 3376) ULaval-CNRS, Biology Department,  
7 Laval University, 1045 Avenue de la Médecine, Québec, QC, Canada G1V 0A6

8 <sup>2</sup> LIENSs, UMR 7266, CNRS-La Rochelle Université, 2 Rue Olympe de Gouges, 17000 La  
9 Rochelle, France

10 <sup>3</sup> LOCEAN, UMR 7159, CNRS, MNHN, IRD, Sorbonne-Université, Station Marine de  
11 Concarneau, BP225, 29900, Concarneau, France

12 <sup>4</sup> Biology Department, Acadia University, 15 University Avenue, Wolfville, NS, B4P 2R6, Canada

13 <sup>5</sup> Environment and Climate Change Canada, National Wildlife Research Centre, Carleton  
14 University, Raven Road, Ottawa, ON, K1A 0H3, Canada

15

16 \* Co-first author

17 <sup>a</sup>Corresponding author: Fanny Cusset (cussetfanny@gmail.com), Julie Charrier  
18 (julie.charrier@univ-lr.fr)

19

20 **ABSTRACT**

21 Sea ice plays a fundamental role in Arctic marine environments, by driving primary productivity  
22 and sustaining ice-associated ecosystems. Simultaneously, sea ice influences the contamination of  
23 Arctic marine organisms, by modifying contaminant cycles or their bioavailability. Changes in sea  
24 ice conditions could therefore profoundly impact the functioning of Arctic marine food webs and  
25 their contamination. Top predators such as seabirds, which are subject to bioaccumulation and  
26 biomagnification of contaminants, are particularly exposed. In this context, the present study aims  
27 to investigate the influence of sea ice and of the use of ice-derived resources on the contamination  
28 of seabirds by mercury (Hg). To this end, eggs of thick-billed murre (Brünnich's guillemots, *Uria*  
29 *lomvia*;  $n = 60$ ) were collected on Prince Leopold Island (Canadian High Arctic) during four years  
30 of varying ice conditions (2010–2013). Trophic tracers (*i.e.*, Highly Branched Isoprenoids, HBIs  
31 – an indicator of the use of ice-derived resources; carbon and nitrogen stable isotopes – indicators  
32 of foraging habitats and trophic status), as well as total Hg concentrations were quantified. Results  
33 showed that feeding on ice-derived resources (as indicated by HBI concentrations) was positively  
34 correlated to sea ice cover, and both positively influenced Hg concentrations in murre eggs.  
35 However, when testing for the best predictor with model selection, sea ice concentration only  
36 drove Hg contamination in murre. This work provides new insights into the role of sea ice and  
37 ice-derived resources in the contamination by Hg of Arctic wildlife. Further research is now  
38 needed to better understand the relationship between sea ice and Hg contamination in Arctic biota  
39 and its underlying mechanisms, but also to identify Hg sources in rapidly changing environmental  
40 conditions in the Arctic.

41 **KEYWORDS**

42 Brünnich's guillemot – Hg – Highly Branched Isoprenoids – Sea ice – Sympagic food web –  
43 Thick-billed murre

44

#### 45 **FUNDING SOURCES**

46 Funding for sample collections was provided by Environment and Climate Change Canada, the  
47 Northern Contaminants Program of Crown-Indigenous Relations and Northern Affairs Canada and  
48 Acadia University. FC benefited from scholarships from Natural Sciences and Engineering  
49 Research Council (Discovery grant to GM). JC is funded by the project ARCTIC-STRESSORS  
50 (French National Research Agency; ANR- 20- CE34- 0006 to JF). The preparation of this paper  
51 was supported by the Sentinel North program of Laval University, made possible, in part thanks  
52 to funding from the Canada First Research Excellence Fund.

## 53 1. INTRODUCTION

54 Sea ice plays a fundamental role in shaping Arctic ecosystems, by driving the phenology of marine  
55 primary production. During spring, melting sea-ice drives several consecutive blooms of primary  
56 producers. In early spring, while ocean surface waters are still covered by ice, a bloom of ice algae  
57 represents a major contributor to the total primary production. This can represent up to 57% of the  
58 entire primary production in the water column and sea ice in the central Arctic (Gosselin et al.,  
59 1997), which constitutes the first levels of sympagic (*i.e.*, ice-associated) food webs. Later, a  
60 bloom of pelagic phytoplankton occurs in ice-free water, supporting pelagic food webs (Horner  
61 and Schrader, 1982; Tremblay et al., 2012). These two consecutive blooms and their phenology  
62 are crucial for secondary production and the functioning of entire marine ecosystems in the Arctic,  
63 highlighting the potential impacts of melting sea ice under the influence of global warming  
64 (Wassmann and Reigstad, 2011).

65 In addition, sea ice plays a central role in the biogeochemical cycle of chemical contaminants, in  
66 their bioavailability to marine wildlife, and thus in the contamination of Arctic marine ecosystems.  
67 This is the case for mercury (Hg), a non-essential and toxic metal that represents a major threat to  
68 Arctic wildlife (AMAP, 2021). Mercury is naturally present in the environment, yet anthropogenic  
69 activities release considerable amounts of Hg into the environment (Zhang et al., 2014). Once in  
70 the atmosphere, this highly volatile contaminant travels *via* the global atmospheric circulation and  
71 reaches even the most remote oceanic regions, such as the Arctic Ocean (Dastoor et al., 2022). As  
72 Hg is highly soluble, it reacts with snow, rain and is easily absorbed by particles (Chételat et al.,  
73 2022). Therefore, it may be deposited in all ecosystems, including sea ice, where it can be stored  
74 for long periods of time (Beattie et al., 2014). Melting sea ice thus represents a major route of Hg  
75 deposition to the ocean, where it is assimilated by primary producers and magnifies along the food

76 webs (Campbell et al., 2005). Furthermore, sea ice can influence the Hg cycle by regulating air-  
77 sea exchanges of Hg species (DiMento et al., 2019) and controlling the photochemical  
78 transformation processes of Hg (Zheng et al., 2021). These processes further modify Hg  
79 bioavailability and the contamination of Arctic marine organisms. Sea ice can also drive Hg levels  
80 in marine predators through changes in their trophic ecology and diet. In marine mammals,  
81 different contaminant patterns were observed in different sea ice conditions, which were related to  
82 prey shifts (Gaden and Stern, 2010; McKinney et al., 2009). In seabirds, changing ice conditions  
83 in northern Hudson Bay has resulted in prey shifts (Gaston et al., 2003) toward a higher  
84 consumption of less contaminated prey (Braune et al., 2014; Gaston et al., 2012b). Further, weather  
85 patterns over multiple years influence exposure of Arctic seabirds to Hg (Foster et al. 2019),  
86 presumably due both to deposition but also release or access to Hg already stored in Arctic archives  
87 (e.g., glaciers and permafrost). Understanding how Arctic predators rely on sympagic versus  
88 pelagic food webs is crucial, not only to foresee future impacts of climate change and associated  
89 sea ice melt on ecosystem structure and dynamics, but also because it could largely alter, directly  
90 or indirectly, their exposure to contaminants. This is particularly important for species that are  
91 used in long-term contaminant monitoring programs, so that changes in contaminant burdens can  
92 be interpreted within the context of climate change (Braune et al., 2014).

93 Multi-tracer approaches enable to track and distinguish the fingerprint of primary producers (*i.e.*,  
94 ice algae and pelagic phytoplankton) throughout the entire food web, revealing the dependency of  
95 Arctic consumers to sympagic and pelagic resources (Amiriaux et al., 2021; Kohlbach et al., 2016;  
96 Yurkowski et al., 2020). Highly branched isoprenoids (HBIs) are lipid biomarkers which are  
97 specifically synthesized by a restricted number of diatom species (Belt and Müller, 2013). In the  
98 Arctic, a restricted number of ice-associated diatoms belonging to genera *Haslea* and *Navicula*

99 synthesize IP<sub>25</sub> and diene (a mono- and a di-unsaturated HBI, respectively), which allow the  
100 tracking of a sympagic fingerprint through a food web. In contrast, triene (a tri-unsaturated HBI)  
101 is mainly synthesized by open-water diatom species, allowing for the tracking of a pelagic  
102 fingerprint through a food web (Belt et al., 2013; Brown et al., 2011). In the last decade, these  
103 biomarkers have provided key insights into the association with sympagic and pelagic food webs  
104 in various consumers (e.g. Amiraux et al., 2023; Brown et al., 2013; Brown and Belt, 2012).  
105 Recently, HBIs were combined with carbon ( $\delta^{13}\text{C}$ ) and nitrogen stable isotopes ( $\delta^{15}\text{N}$ ) – which  
106 are commonly used as proxies of predator trophic ecology: the feeding habitat and the diet,  
107 respectively (Kelly, 2000) – to establish an index of sea ice use (i.e., Ice Use Index, Cusset et al.,  
108 2019).

109 In this context, the present study investigated the relationship between sea ice, the use of sympagic  
110 resources and Hg contamination of an Arctic seabird: the thick-billed murre (or Brünnich's  
111 guillemot, *Uria lomvia*, hereafter «murre») breeding in the Canadian high Arctic. Canadian  
112 murre, like other marine top predators, show high levels of Hg (Braune et al., 2015, Bond et al.,  
113 2015; Chastel et al., 2022; Mallory et al., 2015), and rely on sea ice and ice-derived resources when  
114 ice conditions are favorable (Cusset et al., 2019). More specifically, we (i) investigated differences  
115 in Hg concentrations measured in bird eggs (an indicator of female short-term contamination,  
116 Bond and Diamond, 2010) during four years of contrasting ice conditions (between 2010 and  
117 2013), and (ii) evaluated the drivers of egg Hg contamination (i.e., ice association and trophic  
118 ecology of birds). According to previous studies, we expected an increase of egg Hg concentrations  
119 during icier years and hence a positive association between Hg contamination and the reliance on  
120 sympagic resources.

## 121 2. MATERIAL AND METHODS

### 122 2.1. Study area, species and egg collection

123 The present study was carried out on Prince Leopold Island (Lancaster Sound, hereafter “PLI”;  
124 74°N, 90°W; Figure 1). This site represents one of the largest seabird colonies in the Canadian  
125 Arctic, supporting approximately 100,000 pairs of thick-billed murrelets during the breeding season  
126 (Gaston et al., 2012a). On PLI, the breeding season runs as follows: colony attendance in mid-  
127 June, egg formation (one single egg per nest) in the vicinity of the colony (*i.e.*, for 15 days on  
128 average; Gaston and Nettleship, 1981) until laying in early July, hatching in end-July and chick  
129 fledging from late August to September.

130 A total of 60 eggs (15 eggs per year) were collected at the beginning of the breeding season (late  
131 June – early July) each year between 2010 and 2013, under appropriate permits as part of a long-  
132 term monitoring program supported by Environment and Climate Change Canada and the  
133 Northern Contaminants Program (e.g., Braune et al., 2016). Eggs were collected from nests located  
134 on the eastern and southern cliffs of PLI. Eggs were kept cool in the field and shipped to the  
135 National Wildlife Research Centre (NWRC, Ottawa) for processing. Egg contents were  
136 homogenized for 10-20 s using either a stainless steel Sorvall Omni Mixer or a Brinkmann  
137 Polytron homogenizer. Egg homogenates (1-2 g aliquots) were then stored frozen at -40 °C in  
138 acid-rinsed polyethylene vials for chemical analyses.

139 In seabirds, Hg acquired through feeding accumulates over time in the whole body (including liver,  
140 muscle, kidney). In female seabirds, Hg is excreted *via* two pathways: feather moult and egg  
141 formation/laying. Egg Hg could thus result from Hg acquired locally during egg formation in the  
142 Arctic, but also more globally, during the previous wintering in subarctic regions where Arctic



143 seabirds, including murre, can accumulate large concentrations of Hg (Albert et al., 2021).  
144 However, murre are income breeders (*i.e.*, allocation of local nutrient to egg formation; Bond and  
145 Diamond, 2010; Gaston and Hipfner, 2020). Thus, murre eggs from PLI were assumed to reflect  
146 mainly local diet and Hg contamination of females during egg formation (~two weeks).

147

## 148 **2.2. Ice conditions**

149 As a high Arctic colony, PLI is surrounded by a dense sea-ice cover in winter that progressively  
150 breaks up from west to east in spring and summer. Across years, accessibility to open waters for  
151 birds to forage is highly variable, as the ice edge position can range from the colony as far east as  
152 the Lancaster Sound Polynya in northern Baffin Bay (> 250 km) (Gaston et al., 2005). Sea-ice  
153 conditions were considered during four sampling years (from 2010 to 2013). Since weather  
154 patterns over multiple years influence Hg exposure of Arctic birds (Foster et al., 2019), ice  
155 conditions during the previous years were also considered to investigate potential time-lags.  
156 Because murre exhibit a local feeding range (0–150 km; Gaston et al., 2013), Sea Ice  
157 Concentrations (SIC) were calculated daily for the overall breeding season (between May 1 and  
158 August 31), over a 9-year period (2006–2013), in a 100 km radius around PLI. SIC were expressed  
159 as proportion of ice versus open water pixels, using satellite data from the National Oceanic and  
160 Atmospheric Administration dataset  
161 (<ftp://sidads.colorado.edu/DATASETS/NOAA/G02186/shapefiles/4km/>); 4 km resolution raster  
162 images). Since egg formation was the critical phase investigated in this study, SIC were compared  
163 for June 15 over the years. The 4-year target period exhibited an appreciable sea ice gradient during

164 murre egg formation, from highest SIC in 2012 (latest ice break-up) to the lowest SIC in 2011  
165 (earliest ice break-up) as follows: 2012 > 2010 > 2013 > 2011 (Table 1).

166

## 167 **2.3. Chemical analyses**

### 168 **2.3.1. Trophic tracers**

169 Highly Branched Isoprenoid (HBI) analyses were carried out at Laval University (Québec), using  
170 established techniques (Belt et al., 2012), and were published in Cusset et al. (2019). Briefly, egg  
171 aliquots were freeze-dried for 48 h prior to lipid extraction. Internal standards (7-hexylnonadecane  
172 and 9-octylheptadec-8-ene, 10 µL, 9.68 µg/ml each) were added to egg homogenates to quantify  
173 IP<sub>25</sub> and blanks were analysed with each sample set (*n*=14) to guarantee analytical accuracy.  
174 Total lipids were extracted four consecutive times with dichloromethane:methanol mixture (2:1, 3  
175 min vortex, 15 min sonication). Once dried under a gentle stream of N<sub>2</sub>, total lipid extracts were  
176 saponified (4 mL, 5% MeOH/H<sub>2</sub>O, 90/10, 90°C, 1h). Non-saponifiable lipids (NSL) were then  
177 extracted from the saponification mixture by liquid-liquid extraction (hexane, 3 x 2 mL),  
178 evaporated (nitrogen stream < 35°C) and purified using open column chromatography (SiO<sub>2</sub>  
179 50g/g NSL, hexane), to yield an apolar lipid fraction containing HBIs. HBIs were then analyzed  
180 by gas chromatography-mass spectrometry (GC-MS) and quantified by measuring mass spectral  
181 intensities for each HBI (IP<sub>25</sub>: m/z 350.3, diene: m/z 348.3, triene:m/z 346.3). Finally, HBI  
182 relative concentrations were combined into the H-Print index (Brown et al., 2014) using Eq. 1:

$$183 \quad \text{H-Print (\%)} = [\text{triene}/(\text{IP}_{25} + \text{diene} + \text{triene})] \times 100 \quad (\text{Eq. 1})$$

184 where H-Print indicates a range of association to sympagic (low H-Print), mixed (intermediate)  
185 and pelagic (high H-Print) resources.

186 Stable isotope analyses were conducted at the Littoral, Environment and Societies (LIENSs) Joint  
187 Research Unit and its stable isotope facility (La Rochelle) on delipidized samples loaded into tin  
188 cups (0.2 to 0.8 mg dry weight). Results were previously published in Cusset et al. (2019). Briefly,  
189 stable isotope abundances were determined using an elemental analyzer (Flash EA 1112, Thermo  
190 Scientific, Milan, Italy) coupled in continuous flow mode to an isotope ratio mass spectrometer  
191 (Delta V Plus with a ConFlo IV interface, Thermo Scientific, Bremen, Germany). Results are  
192 expressed in the  $\delta$  notation as deviations from standards (Vienna Pee Dee Belemnite for  $\delta^{13}\text{C}$  and  
193  $\text{N}_2$  in air for  $\delta^{15}\text{N}$ ) following the formula:  $\delta^{13}\text{C}$  or  $\delta^{15}\text{N} = [(R_{\text{sample}}/R_{\text{standard}}) - 1] \times 10^3$ , where R is  
194  $^{13}\text{C}/^{12}\text{C}$  or  $^{15}\text{N}/^{14}\text{N}$ , respectively. Replicate measurements of laboratory standards (USGS-61 and  
195 USGS-62) indicated that the measurement uncertainty was  $< 0.15 \text{ ‰}$  for both  $\delta^{15}\text{N}$  and  $\delta^{13}\text{C}$   
196 values. Based on the distinct  $\delta^{13}\text{C}$  signatures of ice algae and phytoplankton in the Arctic (Hobson  
197 et al. 1995),  $\delta^{13}\text{C}$  isotopic values and H-Print were combined to create an index of sea-ice use, the  
198 Ice Use Index (see Cusset et al., 2019 for detailed methodology).

### 199 **2.3.2. Mercury analyses**

200 Analyses of total Hg (thereafter 'Hg') in egg homogenates were carried out at the NWRC (Ottawa)  
201 and were published in Braune et al. (2016). Briefly, samples were homogenized, freeze-dried,  
202 homogenized again and weighed into nickel combustion boats. They were then analysed for Hg  
203 by direct combustion of the solid sample in an oxygen-rich atmosphere (Salvato and Pirola, 1996),  
204 using an Advanced Mercury Analyser (AMA-254, Altec) equipped with an autosampler. Moisture  
205 content was determined by weight loss during freeze-drying. One or two blank samples were

206 analysed with each sample set to determine analytical accuracy, as well as standard reference  
207 materials (SRMSs). Practical detection limits were 0.006 and 0.004  $\mu\text{g/g}$  dry weight for the 2010-  
208 2012 samples and the 2013 samples, respectively. All Hg concentrations are expressed in  $\mu\text{g/g}$  dry  
209 weight (dw). For further analytical details, including reference materials and recoveries, the reader  
210 is referred to Braune et al. (2016).

#### 211 **2.4. Statistical analyses**

212 All statistical analyses and figures were computed using R version 4.0.3 (R Core Team, 2020).  
213 First, inter-annual differences in egg Hg concentrations were tested using one-way ANOVA. Data  
214 homogeneity and residuals normality were checked prior interpretation, using Breush-Pagan  
215 (package «lmtest»; Zeileis and Hothorn, 2002) and Shapiro tests, respectively. In addition,  
216 differences in ice regimes (extensive- *versus* reduced-ice years) were tested using Welch two-  
217 sample t-tests.

218 Then, drivers of egg Hg concentrations were investigated following two steps. First, simple linear  
219 regressions were used to investigate independently the relationships between egg Hg  
220 concentrations and (i) ice concentrations, (ii) ice association (Ice Use Index) and (iii)  $\delta^{15}\text{N}$  values.  
221 Second, we used general linear models (GLMs) to investigate the role of these explanatory  
222 variables and their combination on Hg concentrations in murre eggs («nlme» package; Pinheiro et  
223 al., 2020). Correlations between variables were checked prior to model construction («cor»  
224 function). Explanatory variables were standardized (mean = 0, SD = 1) to facilitate comparison of  
225 effect sizes. Model assumptions were checked visually with diagnostic functions («plot» function).  
226 All potential combinations of variables (Table 2) were subjected to model selection using the  
227 «AICcmodavg» package (Mazerolle, 2020). Models were compared using Akaike's Information

228 Criterion corrected for small sample sizes ( $AIC_c$ ). The model with the lowest  $AIC_c$  value was  
229 selected as the best model (Burnham and Anderson, 2002). Model support was assessed using  
230 Akaike weights ( $w_i$ ), following Johnson and Omland (2004) and model fit was checked by residual  
231 analysis.

232 During data exploration, time-lags were investigated following previous findings (Foster et al.,  
233 2019). Available ice data for the present dataset only dated back to 2006, implying a maximum  
234 time-lag of four years for sea ice (instead of seven years as showed by Foster et al., 2019). Given  
235 the lack of statistical improvement when added in the models, time-lags were excluded from final  
236 analyses.

237

### 238 **3. RESULTS**

#### 239 **3.1. Hg concentrations in changing ice conditions**

240 Analyses of Hg concentrations in eggs varied significantly among years ( $p < 0.0001$ ,  $F_{3,56} = 7.4$ ,  
241 ANOVA) : 2012 ( $1.2 \pm 0.2 \mu\text{g/g}$ ; heavy dense ice) differed from 2011 ( $0.9 \pm 0.2 \mu\text{g/g}$ ; ice-free)  
242 and 2013 ( $1.0 \pm 0.2 \mu\text{g/g}$ ; low ice), and 2010 ( $1.1 \pm 0.2 \mu\text{g/g}$ ; heavy patchy ice) differed from 2011  
243 (Figure S1). Hg concentrations were lower during reduced-ice years (2011 and 2013;  $0.92 \pm 0.19$   
244  $\mu\text{g/g}$ ,  $n=30$ ) than during extensive-ice years (2010 and 2012;  $1.16 \pm 0.23 \mu\text{g/g}$ ,  $n=30$ ) ( $p < 0.0001$ ,  
245  $t_{56.7}=4.6$ , Welch two-sample t-test; Figure S2). Hence, Hg concentrations increased by 30%  
246 between the minimum and maximum ice years (Table 1).

#### 247 **3.2. Drivers of egg Hg contamination in changing ice conditions**

248 Unifactorial analyses showed that Hg concentrations in murre eggs increased linearly with  
249 increasing ice concentrations ( $R^2=0.25$ ,  $p<0.0001$ ,  $y=0.0037x + 0.78$ ), and with increasing Ice Use  
250 Index ( $R^2=0.19$ ,  $p=0.001$ ,  $y=0.082 x + 1.0$ ; Figure 2), but not with  $\delta^{15} N$  values ( $p=0.08$ ) (Figure  
251 3). Multifactorial analyses revealed that the best model only included ice concentrations as an  
252 explanatory variable (Table 2; Figure 4). Effect size for this model was  $-0.14 \pm 0.03$  ( $-0.2$ ,  $-0.08$ ;  
253 Gamma inverse).

254

#### 255 4. DISCUSSION

256 Climate change has a strong impact on sea ice in the Arctic, for instance its distribution, extent,  
257 thickness and phenology (Garcia-Soto et al., 2021). Yet, melting sea ice could in turn play a  
258 significant role in the contamination by Hg of Arctic marine biota and human populations, through  
259 changes in Hg biogeochemistry or modifications of the food web structure (AMAP, 2022; Chételat  
260 et al., 2022). By using a new approach combining multiple trophic tracers, Hg analyses and sea ice  
261 data, we highlighted the influence of sea ice and sympagic food webs on Hg contamination in  
262 murre during the early breeding season.

263 In years with more extensive sea ice, murre eggs contained higher concentrations of Hg (Figure  
264 4). When considering two distinct ice regimes with relatively “warm” (in 2011 and 2013) and  
265 “cold” (in 2010 and 2012) years characterized by reduced and extensive ice cover, respectively,  
266 Hg concentrations were higher during cold years compared to warm ones (Figure S2). These  
267 results are in agreement with previous investigations using different ice metrics (Mallory and  
268 Braune, 2018). Contrasting Hg levels could result from different foraging ecologies and consumed  
269 prey according to ice conditions. The main route of Hg uptake in predators is through their diet

270 (Atwell et al., 1998; Campbell et al., 2005; Power et al., 2002; Thompson et al., 1998). As pursuit-  
271 divers, murrelets at PLI feed extensively on fish, such as Arctic cod (*Boreogadus saida*), capelin  
272 (*Mallotus villosus*) and sandlance (*Ammodytes sp.*), as well as on macrozooplankton, including  
273 amphipods (Hyperiididae and Gammaridae) and copepods (*Calanus spp.*; Gaston and Nettleship,  
274 1981). Higher Hg contamination during extensive ice years could therefore result from predation  
275 on (i) larger prey species which have bioaccumulated more Hg in their tissues and/or (ii) prey with  
276 higher  $\delta^{15}\text{N}$  values resulting in higher Hg contamination (biomagnification; Dietz et al., 1996).  
277 Following this hypothesis, murrelets'  $\delta^{15}\text{N}$  values should directly influence their Hg contamination.  
278 However, there was a weak relationship between egg Hg concentrations and  $\delta^{15}\text{N}$  isotopic values  
279 (Figure 3), suggesting that temporal changes in trophic ecology alone could not explain higher Hg  
280 contamination during icier years, a result consistent with previous findings (Braune et al. 2016,  
281 Moody et al. 2012, Provencher et al. 2012).

282 Alternatively, higher Hg concentrations in murrelets during icy years could be the consequence of a  
283 higher contamination of sympagic food webs, compared to the more pelagic ones. Indeed, our  
284 results showed that egg Hg contamination was positively related to the Ice Use Index (Figure 2),  
285 which reflects bird association with sympagic resources. Hence, murrelets relying more heavily on  
286 ice-derived resources during the early breeding season exhibited higher Hg concentrations. Similar  
287 findings were observed in polar bears (*Ursus maritimus*), which exhibited higher Hg  
288 concentrations when feeding on food webs dominated by sea-ice associated diatoms (Routti et al.  
289 2012). Higher Hg concentrations were also documented in Arctic cod, an emblematic Arctic fish  
290 species that is closely tied to sea ice (Kohlbach et al. 2017). Arctic cod, the main prey of murrelets  
291 in the High Arctic, especially at PLI (Provencher et al., 2012), use under-ice habitats for part of  
292 their life cycle (David et al. 2016, Gradinger & Bluhm 2004), for instance as a refuge to escape

293 visual predators (LeBlanc et al., 2019). Marginal ice zones (MIZ) thus represent an important  
294 foraging ground for murre (Bradstreet and Cross, 1982). Yet, high Hg concentrations were  
295 observed in MIZ, below the productive surface layer (Heimbürger et al. 2015), enhancing Hg  
296 uptake and bioavailability in ice-associated food webs up to top predators and seabirds such as  
297 murre. Consequently, foraging in these productive habitats may also expose murre to higher Hg  
298 in their diet.

299 Sea ice is composed of different semi-solid matrices, such as brines, gases, particles, and biota  
300 (e.g., bacteria, viruses, algae). These matrices are subject to physical, biological, and chemical  
301 processes which could influence Hg contamination in Arctic marine ecosystems during years of  
302 extensive ice (Steffen et al., 2008; Thomas and Dieckmann, 2009). Sea-ice permeability, shaped  
303 by temperatures and the creation of brine pockets and drainage channels, considerably influences  
304 Hg processes through changing redox conditions and the presence of sea-ice biota (Thomas and  
305 Dieckmann, 2009). Indeed, Hg methylation has been documented in sea ice (Beattie et al., 2014)  
306 and Hg concentrations were the highest in brines (Chaulk et al., 2011), which represent the primary  
307 habitat for microbial communities that sustain sympagic food webs (Thomas and Dieckmann,  
308 2002). Brines provide more Hg-enriched environments for primary producers (Schartup et al.  
309 2020), including ice algae, potentially increasing food web contamination (Stern et al. 2012). Sea  
310 ice could act as an important entry point for Hg at the base of sympagic food webs, additionally  
311 enhancing murre Hg contamination when relying on sympagic resources. Thus, sources of Hg  
312 found in murre eggs could either originate from melting sea ice and snow where Hg can be stored  
313 (Zdanowicz et al., 2013) or from air-ocean exchanges of Hg species (Lalonde et al., 2002; Poulain  
314 et al., 2007).



315 Despite the existing relationship between Hg contamination in murre eggs and their use of  
316 sympagic resources, model selection revealed that the best predictor for egg Hg concentrations  
317 was sea ice concentration only, and did not include the Ice Use Index nor the  $\delta^{15}\text{N}$ . This suggests  
318 that the processes involved are more complex than the reliance on sympagic resources alone. Hg  
319 contamination in murrees can result from long-term processes with a timescale of years, decades  
320 and even centuries (UNEP, 2018). For instance, environmental factors such as the North Atlantic  
321 Oscillation (NAO), snow cover or air temperatures were previously identified as drivers of Hg  
322 contamination in murre eggs, with a lag time of several years (Foster et al., 2019). Mercury can  
323 indeed remain up to one year in the atmosphere (Streets et al., 2019), before deposition and its  
324 resulting methylation, assimilation and final transfer along the food chain. Mercury dynamics are  
325 driven by a large number of interacting post-depositional processes, which control the transport,  
326 methylation and biological uptake of Hg stored in the Arctic Ocean (Dastoor et al., 2022; Outridge  
327 et al., 2008). Thus, reduced sea ice cover or earlier ice break-up may expose murrees to lower Hg  
328 contamination if this was the only change underway. However, air and ocean warming actually  
329 increase local export of Hg to Arctic marine areas from environmental archives found largely on  
330 land (Chételat et al., 2022; Dastoor et al., 2022). For this reason, it is difficult to disentangle all the  
331 processes involved here and one might expect a period of flux and unpredictability, at least until  
332 Arctic Hg archives decrease their contribution to marine environments.

333 Considering its long half-life, Hg is highly persistent in the body of living organisms. Although  
334 eggs mainly reflect local diet and Hg contamination in income-breeders like murrees (i.e., in the  
335 Arctic, during egg formation), they could also integrate, to a low extent, Hg accumulated outside  
336 the Arctic (i.e., during the non-breeding season) and remobilized from storing tissues during egg  
337 synthesis. Previous studies have reported carry-over effects of adult winter contamination on the

338 subsequent summer Hg concentrations in blood of little auks (Carravieri et al., 2023), as well as  
339 higher Hg contamination during the non-breeding season relative to the breeding season in many  
340 alcids, including thick-billed murre (Albert et al., 2021). Future research should now further  
341 investigate how the reliance of Arctic seabirds to ice-derived resources during the non-breeding  
342 season can expose them to Hg and other chemical contaminants.

343

## 344 **5. CONCLUSION**

345 Sea ice is a key component of Arctic marine environments, where it drives primary productivity  
346 and shape the phenology of ice algae and pelagic phytoplankton. At the base of Arctic food webs,  
347 these primary producers provide the vital energy pulses for the entire marine food web to thrive.  
348 Simultaneously, they assimilate contaminants, such as Hg, which are then transferred to all  
349 consumers and predators along the food web. In this study, association with sea ice, and more  
350 particularly the reliance on sympagic resources, was positively related to Hg concentrations in  
351 eggs of thick-billed murre from the Canadian High Arctic. This work provides new insights into  
352 the role of sea ice and ice-derived resources in Hg contamination for Arctic wildlife and human  
353 populations that heavily depend on marine resources for subsistence. Further research is now  
354 required to fully understand the role of ice-derived resources and sea-ice melt in future Hg  
355 contamination of Arctic biota under climate change, as well as the ecological and biogeochemical  
356 interactions involved.

357

358

359 **ACKNOWLEDGMENTS**

360 The authors are thankful to the numerous people involved in field work over the years. Logistical  
361 support for the fieldwork out of Resolute Bay was provided by the Polar Continental Shelf Program  
362 of Natural Resources Canada. Special thanks are due to Caroline Guilmette for her support during  
363 HBI analyses, and to Céline Albert and Alice Carravieri for statistical guidance during data  
364 analyses. We acknowledge the use of the NOAA satellite dataset. This study also represents a  
365 contribution to the French Polar Institute ADACLIM research program (IPEV Pgr 388).

366

367 **ADDITIONAL INFORMATION**

368 **Competing of interest.** Authors have no conflict of interest to declare.

369 **Contributions.**

370 Conception and design: FC, JF, GM, MM

371 Laboratory work and data acquisition: FC (trophic tracers, ice parameters), BB (mercury), GG  
372 (stable isotopes) and PM (ice analyses)

373 Data analysis: FC

374 Interpretation: FC, JC, JF, GM, MM, JP

375 First draft: FC, JC

376 Supervision: GM, JF

377 Revision and final approval: FC, JC, GM, MM, BB, JP, GG, PM, JF

378

379 **REFERENCES**

- 380 Albert, C., Helgason, H.H., Brault-Favrou, M., Robertson, G.J., Descamps, S., Amélineau, F.,  
 381 Danielsen, J., Dietz, R., Elliott, K., Erikstad, K.E., Eulaers, I., Ezhov, A., Fitzsimmons,  
 382 M.G., Gavrilov, M., Golubova, E., Grémillet, D., Hatch, S., Hufféldt, N.P., Jakubas, D.,  
 383 Kitaysky, A., Kolbeinsson, Y., Krasnov, Y., Lorentsen, S.-H., Lorentzen, E., Mallory,  
 384 M.L., Merkel, B., Merkel, F.R., Montevecchi, W., Mosbech, A., Olsen, B., Orben, R.A.,  
 385 Patterson, A., Provencher, J., Plumejeaud, C., Pratte, I., Reiertsen, T.K., Renner, H., Rojek,  
 386 N., Romano, M., Strøm, H., Systad, G.H., Takahashi, A., Thiebot, J.-B., Thórarinsson,  
 387 T.L., Will, A.P., Wojczulanis-Jakubas, K., Bustamante, P., Fort, J., 2021. Seasonal  
 388 variation of mercury contamination in Arctic seabirds: A pan-Arctic assessment. *Sci Total*  
 389 *Environ.* 750, 142201. <https://doi.org/10.1016/j.scitotenv.2020.142201>
- 390 AMAP, 2021. AMAP Assessment 2021: Mercury in the Arctic. Arctic Monitoring and Assessment  
 391 Programme (AMAP), Tromsø, Norway. viii + 324pp
- 392 Amiraux, R., Archambault, P., Moriceau, B., Lemire, M., Babin, M., Memery, L., Massé, G.,  
 393 Tremblay, J.-E., 2021. Efficiency of sympagic-benthic coupling revealed by analyses of n-  
 394 3 fatty acids, IP<sub>25</sub> and other highly branched isoprenoids in two filter-feeding Arctic benthic  
 395 molluscs: *Mya truncata* and *Serripes groenlandicus*. *Org. Geochem.* 151, 104160.  
 396 <https://doi.org/10.1016/j.orggeochem.2020.104160>
- 397 Amiraux, R., Mundy, C.J., Pierrejean, M., Niemi, A., Hedges, K.J., Brown, T.A., Ehn, J.K., Elliott,  
 398 K.H., Ferguson, S.H., Fisk, A.T., Gilchrist, G., Harris, L.N., Iken, K., Jacobs, K.B.,  
 399 Johnson, K.F., Kuzyk, Z.A., Limoges, A., Loewen, T.N., Love, O.P., Matthews, C.J.D.,  
 400 Ogloff, W.R., Rosenberg, B., Søreide, J.E., Watt, C.A., Yurkowski, D.J., 2023. Tracing  
 401 carbon flow and trophic structure of a coastal Arctic marine food web using highly  
 402 branched isoprenoids and carbon, nitrogen and sulfur stable isotopes. *Ecol. Indic.* 147,  
 403 109938. <https://doi.org/10.1016/j.ecolind.2023.109938>
- 404 Atwell, L., Hobson, K.A., Welch, H.E., 1998. Biomagnification and bioaccumulation of mercury  
 405 in an Arctic marine food web: Insights from stable nitrogen isotope analysis 55, 8.
- 406 Beattie, S.A., Armstrong, D., Chaulk, A., Comte, J., Gosselin, M., Wang, F., 2014. Total and  
 407 methylated mercury in Arctic multiyear sea ice. *Environ. Sci. Technol.* 48, 5575–5582.  
 408 <https://doi.org/10.1021/es5008033>
- 409 Belt, S.T., Brown, T.A., Ringrose, A.E., Cabedo-Sanz, P., Mundy, C.J., Gosselin, M., Poulin, M.,  
 410 2013. Quantitative measurement of the sea ice diatom biomarker IP<sub>25</sub> and sterols in Arctic  
 411 sea ice and underlying sediments: Further considerations for palaeo sea ice reconstruction.  
 412 *Org. Geochem.* 62, 33–45. <https://doi.org/10.1016/j.orggeochem.2013.07.002>
- 413 Belt, S.T., Brown, T.A., Rodriguez, A.N., Sanz, P.C., Tonkin, A., Ingle, R., 2012. A reproducible  
 414 method for the extraction, identification and quantification of the Arctic sea ice proxy IP<sub>25</sub>  
 415 from marine sediments. *Anal. Methods* 4, 705–713. <https://doi.org/10.1039/C2AY05728J>

- 416 Belt, S.T., Müller, J., 2013. The Arctic sea ice biomarker IP<sub>25</sub>: A review of current understanding,  
417 recommendations for future research and applications in palaeo sea ice reconstructions.  
418 Quat. Sci. Rev. 79, 9–25. <https://doi.org/10.1016/j.quascirev.2012.12.001>
- 419 Bond, A.L., Diamond, A.W., 2010. Nutrient allocation for egg production in six Atlantic seabirds.  
420 Can. J. Zool. 88, 1095–1102. <https://doi.org/10.1139/Z10-082>
- 421 Bond, A.L., Hobson, K.A., Branfireun, B.A., 2015. Rapidly increasing methyl mercury in  
422 endangered ivory gull (*Pagophila eburnea*) feathers over a 130 year record. Proc. R. Soc.  
423 B. 282:20150032. <http://doi.org/10.1098/rspb.2015.0032>
- 424 Bradstreet, M.S.W., Cross, W.E., 1982. Trophic relationships at High Arctic ice edges. Arctic 35,  
425 1–12.
- 426 Braune, B., Chételat, J., Amyot, M., Brown, T., Clayden, M., Evans, M., Fisk, A., Gaden, A.,  
427 Girard, C., Hare, A., Kirk, J., Lehnherr, I., Letcher, R., Loseto, L., Macdonald, R., Mann,  
428 E., McMeans, B., Muir, D., O'Driscoll, N., Poulain, A., Reimer, K., Stern, G., 2015.  
429 Mercury in the marine environment of the Canadian Arctic: Review of recent findings. Sci.  
430 Total Environ., Special Issue: Mercury in Canada's North 509–510, 67–90.  
431 <https://doi.org/10.1016/j.scitotenv.2014.05.133>
- 432 Braune, B.M., Gaston, A.J., Elliott, K.H., Provencher, J.F., Woo, K.J., Chambellant, M., Ferguson,  
433 S.H., Letcher, R.J., 2014. Organohalogen contaminants and total mercury in forage fish  
434 preyed upon by thick-billed murre in northern Hudson Bay. Mar. Pollut. Bull. 78, 258–  
435 266. <https://doi.org/10.1016/j.marpolbul.2013.11.003>
- 436 Braune, B.M., Gaston, A.J., Mallory, M.L., 2016. Temporal trends of mercury in eggs of five  
437 sympatrically breeding seabird species in the Canadian Arctic. Environ. Pollut. 214, 124–  
438 131. <https://doi.org/10.1016/j.envpol.2016.04.006>
- 439 Brown, T.A., Belt, S.T., 2012. Identification of the sea ice diatom biomarker IP<sub>25</sub> in Arctic benthic  
440 macrofauna: Direct evidence for a sea ice diatom diet in Arctic heterotrophs. Polar Biol.  
441 35, 131–137. <https://doi.org/10.1007/s00300-011-1045-7>
- 442 Brown, T.A., Belt, S.T., Philippe, B., Mundy, C.J., Massé, G., Poulin, M., Gosselin, M., 2011.  
443 Temporal and vertical variations of lipid biomarkers during a bottom ice diatom bloom in  
444 the Canadian Beaufort Sea: Further evidence for the use of the IP<sub>25</sub> biomarker as a proxy  
445 for spring Arctic sea ice. Polar Biol. 34, 1857–1868. <https://doi.org/10.1007/s00300-010-0942-5>
- 447 Brown, T.A., Bicknell, A.W.J., Votier, S.C., Belt, S.T., 2013. Novel molecular fingerprinting of  
448 marine avian diet provides a tool for gaining insights into feeding ecology. Environ. Chem.  
449 Lett. 11, 283–288. <https://doi.org/10.1007/s10311-013-0402-x>
- 450 Burnham, K.P., Anderson, D.R., 2002. Model selection and multimodel inference: A practical  
451 information 616 - Theoretic approach, 2nd ed. Springer US.

- 452 Campbell, L.M., Norstrom, R.J., Hobson, K.A., Muir, D.C.G., Backus, S., Fisk, A.T., 2005a.  
453 Mercury and other trace elements in a pelagic Arctic marine food web (Northwater  
454 Polynya, Baffin Bay). *Sci. Total Environ.*, 351–352, 247–263.  
455 <https://doi.org/10.1016/j.scitotenv.2005.02.043>
- 456 Carravieri, A., Lorient, S., Angelier, F., Chastel, O., Albert, C., Bråthen, V.S., Brisson-Curadeau,  
457 É., Clairbaux, M., Delord, K., Giraudeau, M., Perret, S., Poupart, T., Ribout, C., Viricel-  
458 Pante, A., Grémillet, D., Bustamante, P., Fort, J. 2023. Carryover effects of winter mercury  
459 contamination on summer concentrations and reproductive performance in little auks,  
460 *Environ. Pollut.*, 318, 120774, ISSN 0269-7491.  
461 <https://doi.org/10.1016/j.envpol.2022.120774>.
- 462 Chastel, O., Fort, J., Ackerman, J.T., Albert, C., Angelier, F., Basu, N., Blévin, P., Brault-Favrou,  
463 M., Bustnes, J.O., Bustamante, P., Danielsen, J., Descamps, S., Dietz, R., Erikstad, K.E.,  
464 Eulaers, I., Ezhov, A., Fleishman, A.B., Gabrielsen, G.W., Gavrilov, M., Gilchrist, G., Gilg,  
465 O., Gíslason, S., Golubova, E., Goutte, A., Grémillet, D., Hallgrímsson, G.T., Hansen, E.S.,  
466 Hanssen, S.A., Hatch, S., Huffeldt, N.P., Jakubas, D., Jónsson, J.E., Kitaysky, A.S.,  
467 Kolbeinsson, Y., Krasnov, Y., Letcher, R.J., Linnebjerg, J.F., Mallory, M., Merkel, F.R.,  
468 Moe, B., Montevecchi, W.J., Mosbech, A., Olsen, B., Orben, R.A., Provencher, J.F.,  
469 Ragnarsdóttir, S.B., Reiertsen, T.K., Rojek, N., Romano, M., Søndergaard, J., Strøm, H.,  
470 Takahashi, A., Tartu, S., Thórarinnsson, T.L., Thiebot, J.-B., Will, A.P., Wilson, S.,  
471 Wojczulanis-Jakubas, K., Yannic, G., 2022. Mercury contamination and potential health  
472 risks to Arctic seabirds and shorebirds. *Sci. Total Environ.* 156944.  
473 <https://doi.org/10.1016/j.scitotenv.2022.156944>
- 474 Chaulk, A., Stern, G.A., Armstrong, D., Barber, D.G., Wang, F., 2011. Mercury distribution and  
475 transport across the ocean–sea-ice–atmosphere interface in the Arctic Ocean. *Environ. Sci.*  
476 *Technol.* 45, 1866–1872. <https://doi.org/10.1021/es103434c>
- 477 Chételat, J., McKinney, M.A., Amyot, M., Dastoor, A., Douglas, T.A., Heimbürger-Boavida, L.-  
478 E., Kirk, J., Kahilainen, K.K., Outridge, P.M., Pelletier, N., Skov, H., St. Pierre, K.,  
479 Vuorenmaa, J., Wang, F., 2022. Climate change and mercury in the Arctic: Abiotic  
480 interactions. *Sci. Total Environ.* 824, 153715.  
481 <https://doi.org/10.1016/j.scitotenv.2022.153715>
- 482 Cusset, F., Fort, J., Mallory, M., Braune, B., Massicotte, P., Massé, G., 2019. Arctic seabirds and  
483 shrinking sea-ice: Egg analyses reveal the importance of ice-derived resources. *Sci. Rep.*  
484 9, 1–15. <https://doi.org/10.1038/s41598-019-51788-4>
- 485 Dastoor, A., Angot, H., Bieser, J., Christensen, J.H., Douglas, T.A., Heimbürger-Boavida, L.-E.,  
486 Jiskra, M., Mason, R.P., McLagan, D.S., Obrist, D., Outridge, P.M., Petrova, M.V.,  
487 Ryjkov, A., St. Pierre, K.A., Schartup, A.T., Soerensen, A.L., Toyota, K., Travníkov, O.,  
488 Wilson, S.J., Zdanowicz, C., 2022a. Arctic mercury cycling. *Nat. Rev. Earth Environ.* 3,  
489 270–286. <https://doi.org/10.1038/s43017-022-00269-w>
- 490 Dastoor, A., Angot, H., Bieser, J., Christensen, J.H., Douglas, T.A., Heimbürger-Boavida, L.-E.,  
491 Jiskra, M., Mason, R.P., McLagan, D.S., Obrist, D., Outridge, P.M., Petrova, M.V.,

- 492 Ryjkov, A., St. Pierre, K.A., Schartup, A.T., Soerensen, A.L., Toyota, K., Travnikov, O.,  
493 Wilson, S.J., Zdanowicz, C., 2022b. Arctic mercury cycling. *Nat. Rev. Earth Environ.* 3,  
494 270–286. <https://doi.org/10.1038/s43017-022-00269-w>
- 495 David, C., Lange, B., Krumpfen, T., Schaafsma, F., van Franeker, J.A., Flores, H., 2016. Under-ice  
496 distribution of polar cod *Boreogadus saida* in the central Arctic Ocean and their association  
497 with sea-ice habitat properties. *Polar Biol.* 39, 981–994. <https://doi.org/10.1007/s00300-015-1774-0>  
498
- 499 Dietz, R., Letcher, R.J., Aars, J., Andersen, M., Boltunov, A., Born, E.W., Ciesielski, T.M., Das,  
500 K., Dastnai, S., Derocher, A.E., Desforges, J.-P., Eulaers, I., Ferguson, S., Hallanger, I.G.,  
501 Heide-Jørgensen, M.P., Heimbürger-Boavida, L.-E., Hoekstra, P.F., Jenssen, B.M.,  
502 Kohler, S.G., Larsen, M.M., Lindstrøm, U., Lippold, A., Morris, A., Nabe-Nielsen, J.,  
503 Nielsen, N.H., Peacock, E., Pinzone, M., Rigét, F.F., Rosing-Asvid, A., Routti, H., Siebert,  
504 U., Stenson, G., Stern, G., Strand, J., Søndergaard, J., Treu, G., Víkingsson, G.A., Wang,  
505 F., Welker, J.M., Wiig, Ø., Wilson, S.J., Sonne, C., 2022. A risk assessment review of  
506 mercury exposure in Arctic marine and terrestrial mammals. *Sci. Total Environ.* 829,  
507 154445. <https://doi.org/10.1016/j.scitotenv.2022.154445>
- 508 Dietz, R., Rigét, F., Johansen, P., 1996. Lead, cadmium, mercury and selenium in Greenland  
509 marine animals. *Sci. Total Environ.* 186, 67–93. [https://doi.org/10.1016/0048-9697\(96\)05086-3](https://doi.org/10.1016/0048-9697(96)05086-3)  
510
- 511 DiMento, B.P., Mason, R.P., Brooks, S., Moore, C., 2019. The impact of sea ice on the air-sea  
512 exchange of mercury in the Arctic Ocean. *Deep Sea Res. Part Oceanogr. Res. Pap.* 144,  
513 28–38. <https://doi.org/10.1016/j.dsr.2018.12.001>
- 514 Foster, K.L., Braune, B.M., Gaston, A.J., Mallory, M.L., 2019. Climate influence on mercury in  
515 Arctic seabirds. *Sci. Total Environ.* 693, 133569.  
516 <https://doi.org/10.1016/j.scitotenv.2019.07.375>
- 517 Garcia-Soto, C., Cheng, L., Caesar, L., Schmidtko, S., Jewett, E.B., Cheripka, A., Rigor, I.,  
518 Caballero, A., Chiba, S., Báez, J.C., Zielinski, T., Abraham, J.P., 2021. An overview of  
519 ocean climate change indicators: Sea surface temperature, ocean heat content, ocean pH,  
520 dissolved oxygen concentration, Arctic sea ice extent, thickness and volume, sea level and  
521 strength of the AMOC (Atlantic Meridional Overturning Circulation). *Front. Mar. Sci.* 8,  
522 642372. <https://doi.org/10.3389/fmars.2021.642372>
- 523 Gaston, A.J., Elliott, K.H., Ropert-Coudert, Y., Kato, A., Macdonald, C.A., Mallory, M.L.,  
524 Gilchrist, H.G., 2013. Modeling foraging range for breeding colonies of thick-billed murre  
525 *Uria lomvia* in the Eastern Canadian Arctic and potential overlap with industrial  
526 development. *Biol. Conserv.* 168, 134–143. <https://doi.org/10.1016/j.biocon.2013.09.018>
- 527 Gaston, A.J., Gilchrist, H.G., Mallory, M.L., 2005. Variation in ice conditions has strong effects  
528 on the breeding of marine birds at Prince Leopold Island, Nunavut. *Ecography* 28, 331–  
529 344. <https://doi.org/10.1111/j.0906-7590.2005.04179.x>

- 530 Gaston, A. J., & Hipfner, J. M. (2020). Thick-billed Murre (*Uria lomvia*), version 1.0. In Birds of  
531 the World (S. M. Billerman, Editor). Cornell Lab of Ornithology, Ithaca, NY, USA.  
532 <https://doi.org/10.2173/bow.thbmur.01>
- 533 Gaston, A.J., Mallory, M.L., Gilchrist, H.G., 2012a. Populations and trends of Canadian Arctic  
534 seabirds. Polar Biol. 35, 1221–1232. <https://doi.org/10.1007/s00300-012-1168-5>
- 535 Gaston, A.J., Nettleship, D.N., 1981. The thick-billed murre of Prince Leopold Island, Monograph  
536 Series. Environment Canada - Canadian Wildlife Service, Ottawa.
- 537 Gaston, A.J., Smith, P.A., Provencher, J.F., 2012b. Discontinuous change in ice cover in Hudson  
538 Bay in the 1990s and some consequences for marine birds and their prey. ICES J. Mar. Sci.  
539 69, 1218–1225. <https://doi.org/10.1093/icesjms/fss040>
- 540 Gaston, A.J., Woo, K., Hipfner, J.M., 2003. Trends in forage fish populations in Northern Hudson  
541 Bay since 1981, as determined from the diet of nestling thick-billed murrets, *Uria lomvia*.  
542 ARCTIC 56, 227–233. <https://doi.org/10.14430/arctic618>
- 543 Gosselin, M., Levasseur, M., Wheeler, P.A., Horner, R.A., Booth, B.C., 1997. New measurements  
544 of phytoplankton and ice algal production in the Arctic Ocean. Deep Sea Res. Part II Top.  
545 Stud. Oceanogr. 44, 1623–1644. [https://doi.org/10.1016/S0967-0645\(97\)00054-4](https://doi.org/10.1016/S0967-0645(97)00054-4)
- 546 Gradinger, R.R., Bluhm, B.A., 2004. In-situ observations on the distribution and behavior of  
547 amphipods and Arctic cod (*Boreogadus saida*) under the sea ice of the High Arctic Canada  
548 Basin. Polar Biol. 27, 595–603. <https://doi.org/10.1007/s00300-004-0630-4>
- 549 Heimbürger, L.-E., Sonke, J.E., Cossa, D., Point, D., Lagane, C., Laffont, L., Galfond, B.T.,  
550 Nicolaus, M., Rabe, B., van der Loeff, M.R., 2015. Shallow methylmercury production in  
551 the marginal sea ice zone of the central Arctic Ocean. Sci. Rep. 5, 10318.  
552 <https://doi.org/10.1038/srep10318>
- 553 Horner, R., Schrader, G.C., 1982. Relative contributions of ice algae, phytoplankton, and benthic  
554 microalgae to primary production in nearshore regions of the Beaufort Sea. Arctic 35, 485–  
555 503.
- 556 Johnson, J.B., Omland, K.S., 2004. Model selection in ecology and evolution. Trends Ecol. Evol.  
557 19, 101744 108. <https://doi.org/10.1016/j.tree.2003.10.013>
- 558 Kelly, J.F., 2000. Stable isotopes of carbon and nitrogen in the study of avian and mammalian  
559 trophic ecology. Can. J. Zool. 78, 1–27. <https://doi.org/10.1139/z99-165>
- 560 Kohlbach, D., Graeve, M., Lange, B.A., David, C., Peeken, I., Flores, H., 2016. The importance  
561 of ice algae-produced carbon in the central Arctic Ocean ecosystem: Food web  
562 relationships revealed by lipid and stable isotope analyses. Limnol. Oceanogr. 61, 2027–  
563 2044. <https://doi.org/10.1002/lno.10351>
- 564 Kohlbach, D., Schaafsma, F.L., Graeve, M., Lebreton, B., Lange, B.A., David, C., Vortkamp, M.,  
565 Flores, H., 2017. Strong linkage of polar cod (*Boreogadus saida*) to sea ice algae-produced



566 carbon: Evidence from stomach content, fatty acid and stable isotope analyses. *Prog.*  
567 *Oceanogr.* 152, 62–74. <https://doi.org/10.1016/j.pocean.2017.02.003>

568 Lalonde, J.D., Poulain, A.J., Amyot, M., 2002. The role of mercury redox reactions in snow on  
569 snow-to-air mercury transfer. *Environ. Sci. Technol.* 36, 174–178.  
570 <https://doi.org/10.1021/es010786g>

571 LeBlanc, M., Gauthier, S., Garbus, S.E., Mosbech, A., Fortier, L., 2019. The co-distribution of  
572 Arctic cod and its seabird predators across the marginal ice zone in Baffin Bay. *Elem Sci*  
573 *Anth* 7, 1. <https://doi.org/10.1525/elementa.339>

574 Mallory, M.L., Braune, B.M., 2018. Do concentrations in eggs and liver tissue tell the same story  
575 of temporal trends of mercury in high Arctic seabirds? *J. Environ. Sci.* 68, 65–72.  
576 <https://doi.org/10.1016/j.jes.2017.10.017>

577 Mallory, M.L., Braune, B.M., Provencher, J.F., Callaghan, D.B., Gilchrist, H.G., Edmonds, S.T.,  
578 Allard, K., O’Driscoll, N.J., 2015. Mercury concentrations in feathers of marine birds in  
579 Arctic Canada. *Mar. Pollut. Bull.* 98, 308–313.  
580 <https://doi.org/10.1016/j.marpolbul.2015.06.043>

581 Mazerolle, M.J., 2020. AICcmodavg: Model selection and multimodel inference based on  
582 (Q)AIC(c). R package version 2.3-1. <https://cran.r-project.org/package=AICcmodavg>.

583 McKinney, M.A., Peacock, E., Letcher, R.J., 2009. Sea ice-associated diet change increases the  
584 levels of chlorinated and brominated contaminants in polar bears. *Environ. Sci. Technol.*  
585 43, 4334–4339. <https://doi.org/10.1021/es900471g>

586 Outridge, P.M., Macdonald, R.W., Wang, F., Stern, G.A., Dastoor, A.P., 2008. A mass balance  
587 inventory of mercury in the Arctic Ocean. *Environ. Chem.* 5, 89.  
588 <https://doi.org/10.1071/EN08002>

589 Perrette, M., Yool, A., Quartly, G.D., Popova, E.E., 2011. Near-ubiquity of ice-edge blooms in the  
590 Arctic. *Biogeosciences* 8, 515–524. <https://doi.org/10.5194/bg-8-515-2011>

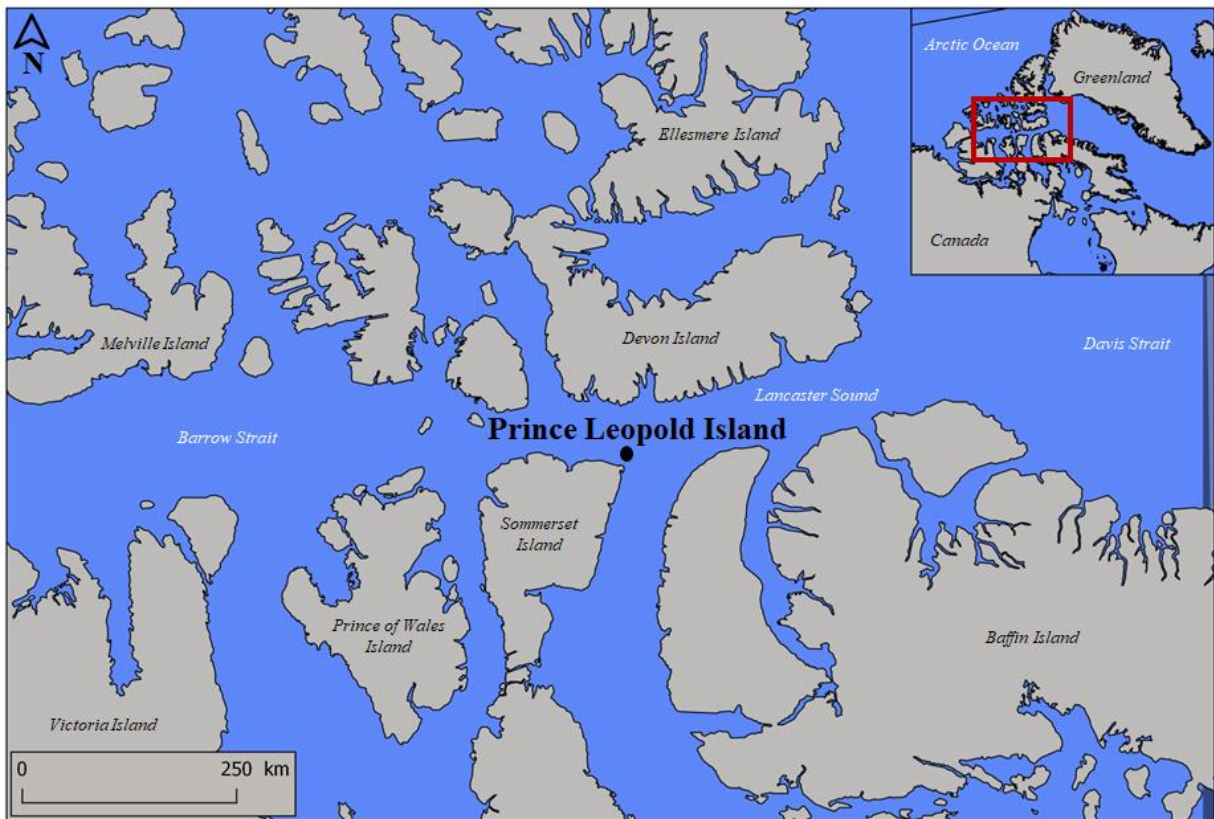
591 Pinheiro, J., Bates, D., DebRoy, S., Sarkar, D., R Core Team, 2020. nlme: Linear and nonlinear  
592 mixed effects models. R package version 3.1-149, [https://CRAN.R-](https://CRAN.R-project.org/package=nlme)  
593 [project.org/package=nlme](https://CRAN.R-project.org/package=nlme)

594 Poulain, A.J., Garcia, E., Amyot, M., Campbell, P.G.C., Raofie, F., Ariya, P.A., 2007. Biological  
595 and chemical redox transformations of mercury in fresh and salt waters of the High Arctic  
596 during spring and summer. *Environ. Sci. Technol.* 41, 1883–1888.  
597 <https://doi.org/10.1021/es061980b>

598 Power, M., Klein, G.M., Guiguer, K.R.R.A., Kwan, M.K.H., 2002. Mercury accumulation in the  
599 fish community of a sub-Arctic lake in relation to trophic position and carbon sources: Hg  
600 in a sub-Arctic lacustrine fish community. *J. Appl. Ecol.* 39, 819–830.  
601 <https://doi.org/10.1046/j.1365-2664.2002.00758.x>

- 602 Provencher, J.F., Gaston, A.J., O'Hara, P.D., Gilchrist, H.G., 2012. Seabird diet indicates changing  
603 Arctic marine communities in eastern Canada. *Mar. Ecol. Prog. Ser.* 454, 171–182.  
604 <https://doi.org/10.3354/meps09299>
- 605 R Core Team, 2020. R: A language an environment for statistical computing. R Foundation for  
606 statistical computing, Vienna, Austria. URL: <https://www.R-project.org/>
- 607 Routti, H., Letcher, R.J., Born, E.W., Branigan, M., Dietz, R., Evans, T.J., McKinney, M.A.,  
608 Peacock, E., Sonne, C., 2012. Influence of carbon and lipid sources on variation of mercury  
609 and other trace elements in polar bears (*Ursus maritimus*). *Environ. Toxicol. Chem.* 31,  
610 2739–2747. <https://doi.org/10.1002/etc.2005>
- 611 Salvato, N., Pirola, C., 1996. Analysis of mercury traces by means of solid sample atomic  
612 absorption spectrometry. *Microchim. Acta* 123, 63–71.  
613 <https://doi.org/10.1007/BF01244379>
- 614 Schartup, A.T., Soerensen, A.L., Heimbürger-Boavida, L.-E., 2020. Influence of the Arctic sea-  
615 ice regime shift on sea-ice methylated mercury trends. *Environ. Sci. Technol. Lett.* 7, 708–  
616 713. <https://doi.org/10.1021/acs.estlett.0c00465>
- 617 Steffèn, A., Douglas, T., Amyot, M., Ariya, P., Aspö, K., Berg, T., Bottenheim, J., Brooks, S.,  
618 Cobbett, F., Dastoor, A., Dommergue, A., Ebinghaus, R., Ferrari, C., Gardfeldt, K.,  
619 Goodsite, M.E., Lean, D., Poulain, A.J., Scherz, C., Skov, H., Sommar, J., Temme, C.,  
620 2008. A synthesis of atmospheric mercury depletion event chemistry in the atmosphere and  
621 snow. *Atmospheric Chem. Phys.* 8, 1445–1482. <https://doi.org/10.5194/acp-8-1445-2008>
- 622 Stern, G.A., Macdonald, R.W., Outridge, P.M., Wilson, S., Chételat, J., Cole, A., Hintelmann, H.,  
623 Loseto, L.L., Steffèn, A., Wang, F., Zdanowicz, C., 2012. How does climate change  
624 influence Arctic mercury? *Sci. Total Environ.* 414, 22–42.  
625 <https://doi.org/10.1016/j.scitotenv.2011.10.039>
- 626 Streets, D.G., Horowitz, H.M., Lu, Z., Levin, L., Thackray, C.P., Sunderland, E.M., 2019. Five  
627 hundred years of anthropogenic mercury: spatial and temporal release profiles\*. *Environ*  
628 *Res Lett* 14:084004. <https://doi.org/10.1088/1748-9326/ab281f>
- 629 Thomas, D.N., Dieckmann, G.S., 2009. *Sea ice*. John Wiley & Sons.
- 630 Thomas, D.N., Dieckmann, G.S., 2002. Antarctic sea ice: A Habitat for extremophiles. *Science*  
631 295, 641–644. <https://doi.org/10.1126/science.1063391>
- 632 Thompson, D.R., Furness, R.W., Monteiro, L.R., 1998. Seabirds as biomonitors of mercury inputs  
633 to epipelagic and mesopelagic marine food chains. *Sci. Total Environ.* 213, 299–305.  
634 [https://doi.org/10.1016/S0048-9697\(98\)00103-X](https://doi.org/10.1016/S0048-9697(98)00103-X)
- 635 Tremblay, J.-É., Robert, D., Varela, D.E., Lovejoy, C., Darnis, G., Nelson, R.J., Sastri, A.R., 2012.  
636 Current state and trends in Canadian Arctic marine ecosystems: I. Primary production.  
637 *Clim. Change* 115, 161–178. <https://doi.org/10.1007/s10584-012-0496-3>

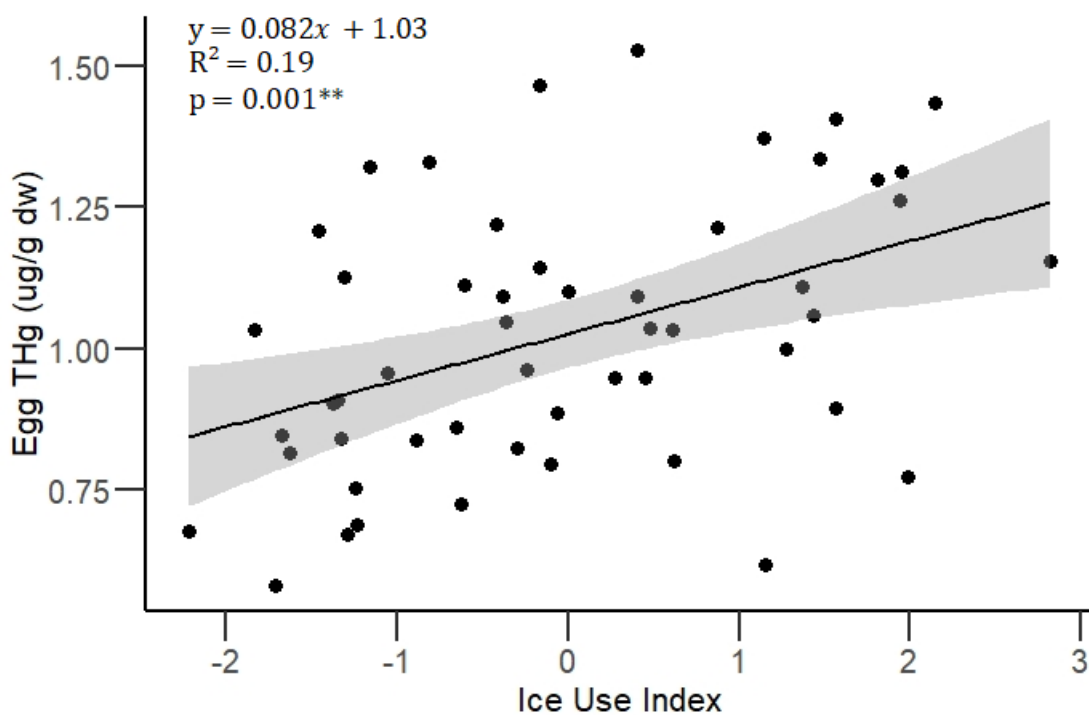
- 638 Wassmann, P., Reigstad, M., 2011. Future Arctic Ocean seasonal ice zones and implications for  
639 pelagic-benthic coupling. *Oceanography* 24, 220–231.  
640 <https://doi.org/10.5670/oceanog.2011.74>
- 641 Yurkowski, D.J., Brown, T.A., Blanchfield, P.J., Ferguson, S.H., 2020. Atlantic walrus signal  
642 latitudinal differences in the long-term decline of sea ice-derived carbon to benthic fauna  
643 in the Canadian Arctic. *Proc. R. Soc. B Biol. Sci.* 287, 20202126.  
644 <https://doi.org/10.1098/rspb.2020.2126>
- 645 Zeileis, A., Hothorn, T., 2002. Diagnostic checking in regression relationships. *R News* 2(3), 7-  
646 10. <https://CRAN.R-project.org/doc/Rnews>
- 647 Zdanowicz, C., Krümmel, E.M., Lean, D., Poulain, A.J., Yumvihoze, E., Chen, J., Hintelmann,  
648 H., 2013. Accumulation, storage and release of atmospheric mercury in a glaciated Arctic  
649 catchment, Baffin Island, Canada. *Geochim. Cosmochim. Acta* 107, 316–335.  
650 <https://doi.org/10.1016/j.gca.2012.11.028>
- 651 Zhang, Y., Jaeglé, L., Thompson, L., Streets, D.G., 2014. Six centuries of changing oceanic  
652 mercury: Anthropogenic mercury in ocean. *Glob. Biogeochem. Cycles* 28, 1251–1261.  
653 <https://doi.org/10.1002/2014GB004939>
- 654 Zheng, W., Chandan, P., Steffen, A., Stupple, G., De Vera, J., Mitchell, C.P.J., Wania, F.,  
655 Bergquist, B.A., 2021. Mercury stable isotopes reveal the sources and transformations of  
656 atmospheric Hg in the high Arctic. *Appl. Geochem.* 131, 105002.  
657 <https://doi.org/10.1016/j.apgeochem.2021.105002>  
658



660

661

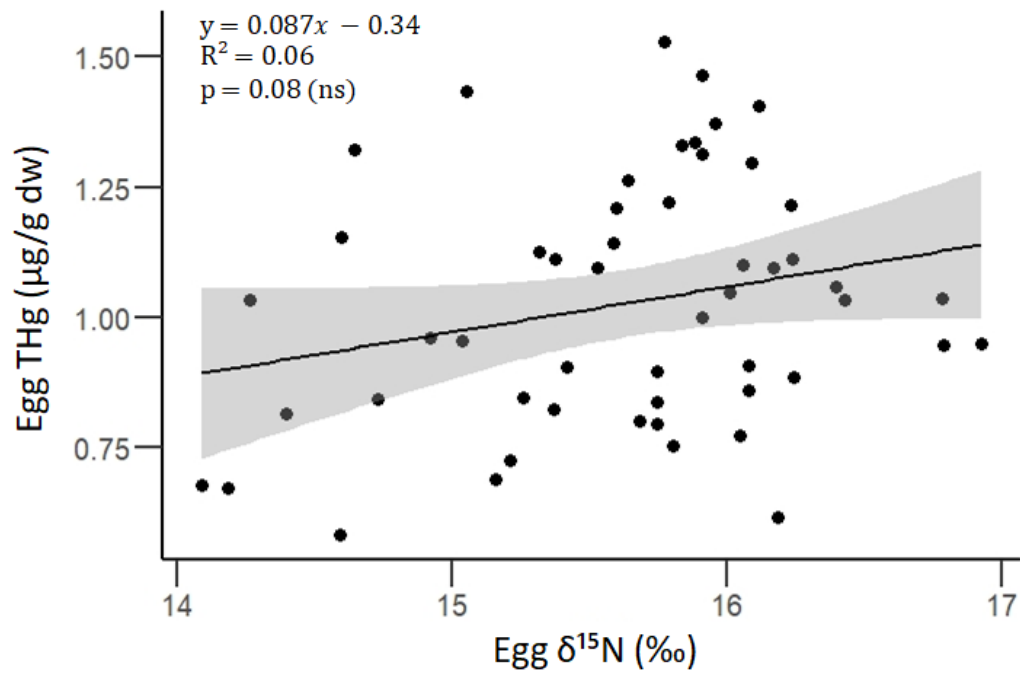
**Figure 1.** Location of Prince Leopold Island in the Canadian High Arctic



662

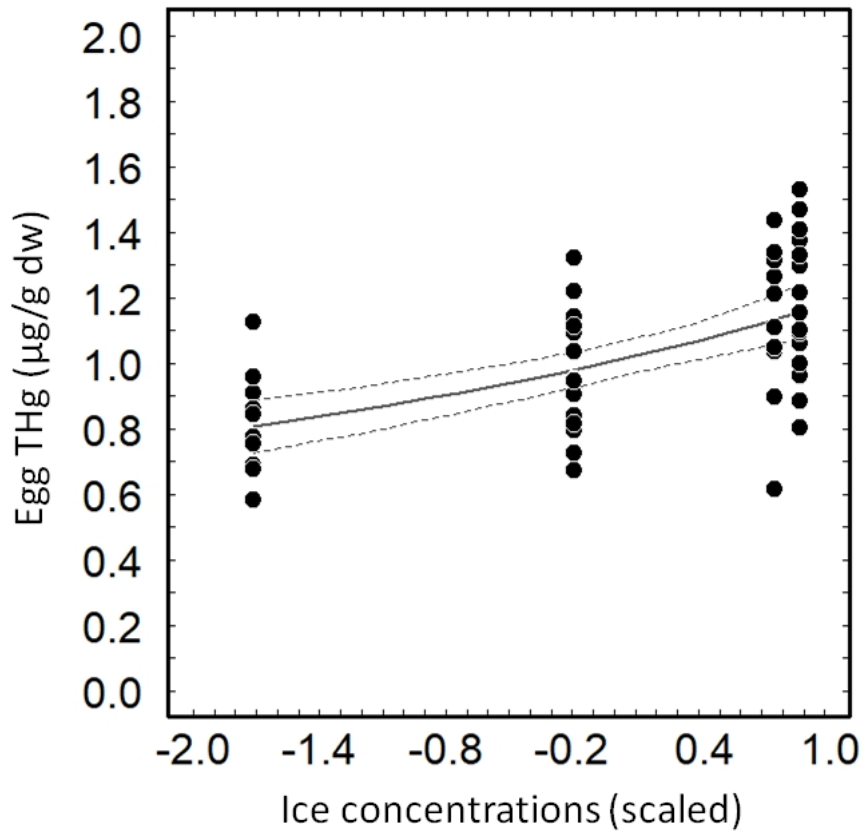
663 **Figure 2.** Relationship between total Hg concentrations measured in eggs of thick-billed murre  
 664 (*Uria lomvia*) from Prince Leopold Island (Nunavut, Canada) and Ice Use Index. Lower and higher  
 665 values of Ice Use Index correspond to the most pelagic and sympagic feeding association,  
 666 respectively.

667



668

669 **Figure 3.** Relationship between total Hg concentrations ( $\mu\text{g/g dw}$ ) measured in eggs of thick-billed  
 670 murre (*Uria lomvia*) from Prince Leopold Island (Nunavut, Canada) and  $\delta^{15}\text{N}$  values (proxy for  
 671 trophic position).



672

673 **Figure 4.** Egg total Hg concentrations of thick-billed murre (*Uria lomvia*) from Prince Leopold  
 674 Island (Nunavut, Canada) with varying ice concentrations. Ice concentrations were scaled for  
 675 statistical analyses (raw concentrations range from 17.02 to 97.96 %). Solid and dotted lines  
 676 represent the best-fitting model detected from construction of Generalized Linear Models (GLMs)  
 677 and the confidence interval, respectively (see “Material and Methods” for further details).

## TABLES

**Table 1.** Ice conditions and egg parameters from thick-billed murre collected between 2010 and 2013 on Prince Leopold Island (Nunavut, Canada): trophic tracers include the Ice Use Index, carbon- ( $\delta^{13}\text{C}$ ) and nitrogen- ( $\delta^{15}\text{N}$ ) stable isotopes; total mercury (THg) concentrations ( $\mu\text{g/g dw}$ ).  $\delta^{13}\text{C}$  and  $\delta^{15}\text{N}$  are proxies for bird feeding habitat and trophic position, respectively. Values represent means  $\pm$  SD (n).

	<i>2010</i>	<i>2011</i>	<i>2012</i>	<i>2013</i>
<b>Ice concentrations<sup>1</sup> (%)</b>	99.0	33.4	99.0	79.8
<b>Ice characteristics<sup>2</sup></b>	Patchy, large floes, leads with water access	Ice-free	Dense pack-ice, no leads, ice edge > 250 km away	Dense pack ice, ice edge 50 km away
<b>Ice Use Index<sup>3</sup></b>	1.0 $\pm$ 1.1 (15)	-1.1 $\pm$ 1.1 (15)	0.7 $\pm$ 1.0 (15)	0.7 $\pm$ 0.7 (15)
<b>H-Print (%)<sup>4</sup></b>	28.1 $\pm$ 20.8 (15)	82.5 $\pm$ 18.8 (15)	56.9 $\pm$ 27.3 (15)	63.4 $\pm$ 18.1 (15)
<b><math>\delta^{13}\text{C}</math> (‰)</b>	-19.7 $\pm$ 0.4 (11)	-20.3 $\pm$ 0.5 (11)	-19.3 $\pm$ 0.4 (15)	-20.3 $\pm$ 0.3 (15)
<b><math>\delta^{15}\text{N}</math> (‰)</b>	16.0 $\pm$ 0.5 (11)	15.3 $\pm$ 0.7 (11)	15.8 $\pm$ 0.5 (15)	15.4 $\pm$ 0.8 (15)
<b>THg (<math>\mu\text{g/g dw}</math>)</b>	1.1 $\pm$ 0.2 (15)	0.9 $\pm$ 0.2 (15)	1.2 $\pm$ 0.2 (15)	1.0 $\pm$ 0.2 (15)
<b>Moisture (%)</b>	73.3 $\pm$ 0.9 (15)	69.1 $\pm$ 2.5 (15)	73.7 $\pm$ 1.0 (15)	73.6 $\pm$ 1.0 (15)

<sup>1</sup>Ice concentrations represent the proportion of sea ice *versus* open water in a 100 km radius around the colony at the time of egg-laying (on June 15). Please refer to the “Material and Methods” for further details.

<sup>2</sup>Despite similar ice concentrations, 2010 and 2012 differed in their ice characteristics. Complete description of ice conditions is available in Cusset et al. (2019).

<sup>3</sup>The Ice Use Index indicates the degree of ice feeding association (values < and > 0 indicates low and high reliance on sympagic resources, respectively).

<sup>4</sup>H-Print (i.e., HBI-fingerprint) indicates the degree of association to ice-derived resources (from 0 to 100% for sympagic and pelagic association, respectively).



**Table 2.** AIC<sub>c</sub> model ranking from statistical analyses of egg THg concentrations from thick-billed murres breeding on Prince Leopold Island (2010-2013). Models are Generalized Linear Models (GLMs) with a Gamma distribution and an inverse link function. Explanatory variables include: ice concentrations within 100 km around the colony («Ice»), the type of association to sea-ice and its derived resources (pelagic *versus* sympagic; «IceUse»), the trophic position (« $\delta^{15} N$ ») and their relevant interactions. Abbreviations: k, the number of parameters; AIC<sub>c</sub>, Akaike’s Information Criteria adjusted for small sample-size values; w<sub>i</sub>, AICc weights (weights across all models sum to 1.00); LL, Log-Likelihood.

<b>Models</b>	<b>k</b>	<b>AIC<sub>c</sub></b>	<b><math>\Delta</math>AIC<sub>c</sub></b>	<b>w<sub>i</sub></b>	<b>LL</b>
<b><i>THg ~ Ice*</i></b>	<b>3</b>	<b>-16.43</b>	<b>0.00</b>	<b>0.83</b>	<b>11.46</b>
<i>THg ~ <math>\delta^{15} N + IceUse + Ice</math></i>	5	-12.79	3.64	0.13	12.05
<i>THg ~ <math>\delta^{15} N + IceUse + \delta^{15} N:IceUse + Ice + Ice :IceUse</math></i>	7	-9.44	6.99	0.03	12.99
<i>THg ~ IceUse</i>	3	-7.04	9.38	0.01	6.77
<i>THg ~ <math>\delta^{15} N + IceUse</math></i>	4	-5.02	11.40	0.00	6.94
<i>THg ~ <math>\delta^{15} N + IceUse + \delta^{15} N:IceUse</math></i>	5	-4.13	12.30	0.00	7.72
<i>THg ~ <math>\delta^{15} N + IceUse + Ice:IceUse</math></i>	5	-2.96	13.46	0.00	7.13
<i>THg ~ <math>\delta^{15} N</math></i>	3	0.18	16.60	0.00	3.16
<i>THg ~ NULL</i>	2	1.14	17.56	0.00	1.55

\*The best model (in bold) is selected with the lowest AIC<sub>c</sub> value.

## **CREDIT AUTHOR STATEMENT**

### **Contributions.**

Conception and design: FC, JF, GM, MM

Laboratory work and data acquisition: FC (trophic tracers, ice parameters), BB (mercury), GG (stable isotopes) and PM (ice analyses)

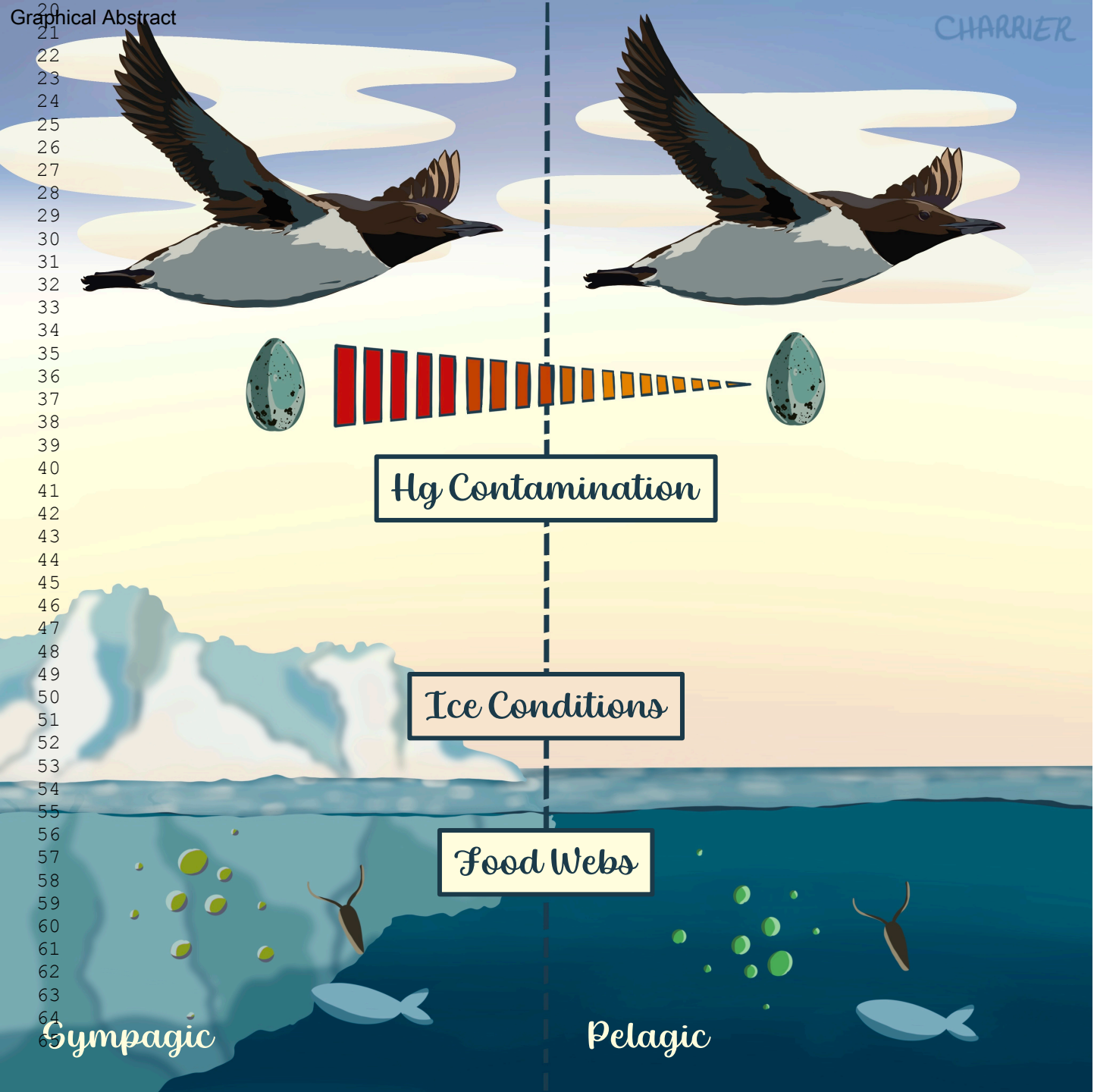
Data analysis: FC

Interpretation: FC, JC, JF, GM, MM, JP

First draft: FC, JC

Supervision: GM, JF

Revision and final approval: FC, JC, GM, MM, BB, JP, GG, PM, JF



Hg Contamination

Ice Conditions

Food Webs

Sympagic

Pelagic